Plant Physiology®

Plant Physiology, 2025, **198**, kiaf163
https://doi.org/10.1093/plphys/kiaf163
Advance access publication 15 May 2025
Research Article

N-hydroxypipecolic acid and salicylic acid play key roles in autoimmunity induced by loss of the callose synthase PMR4

Baofang Fan,[1,†] Zizhang Li,[2,†] Amber Jannasch,[3] Shunyuan Xiao,[2,4] Zhixiang Chen[1,*]

[1]Department of Botany and Plant Pathology, Purdue University, 915 Mitch Daniels Boulevard, West Lafayette, IN 47907, USA
[2]Institute for Bioscience and Biotechnology Research, University of Maryland, Rockville, MD 20850, USA
[3]Metabolomics Profiling Facility, Bindley Bioscience Center, Purdue University, 1203 Mitch Daniels Boulevard, West Lafayette, IN 47907, USA
[4]Department of Plant Science and Landscape Architecture, University of Maryland, College Park, MD 20742, USA
*Author for correspondence: zhixiang@purdue.edu
†These authors contributed equally to the work.
The author responsible for distribution of materials integral to the findings presented in this article in accordance with the policy described in the Instructions for Authors (https://academic.oup.com/plphys/pages/General-Instructions) is: Zhixiang Chen (zhixiang@purdue.edu).

Abstract

In *Arabidopsis thaliana*, the POWDERY MILDEW RESISTANT4 (PMR4)/GLUCAN SYNTHASE LIKE5 (GSL5) callose synthase is required for pathogen-induced callose deposition in cell wall defense. Paradoxically, *pmr4/gsl5* mutants exhibit strong resistance to both powdery and downy mildew. The powdery mildew resistance of *pmr4/gsl5* has been attributed to upregulated salicylic acid (SA) signaling based on its dependance on *PHYTOALEXIN DEFICIENT4* (*PAD4*), which controls SA accumulation, and its abolishment by bacterial NahG salicylate hydroxylase. Our study revealed that disruption of *PMR4/GSL5* also leads to early senescence. Suppressor analysis uncovered that *PAD4* and *N*-hydroxypipecolic acid (NHP) biosynthetic genes *ABERRANT GROWTH AND DEATH2-LIKE DEFENSE RESPONSE PROTEIN1* (*ALD1*) and *FLAVIN-DEPENDENT MONOXYGENASE1* (*FMO1*) are required for early senescence of *pmr4/gsl5* mutants. The critical role of NHP in the early senescence of *pmr4/gsl5* was supported by greatly increased accumulation of pipecolic acid in *pmr4/gsl5* mutants. In contrast, disruption of the SA biosynthetic gene *ISOCHORISMATE SYNTHASE1/SA-INDUCTION DIFFICIENT 2* (*ICS1/SID2*), which greatly reduces SA accumulation, had little effect on impaired growth of *pmr4/gsl5*. Furthermore, while disruption of *PAD4* completely abolished the powdery mildew resistance in *pmr4/gsl5,* mutations in *ICS1/SID2*, *ALD1*, or *FMO1* had only a minor effect on the resistance of the mutant plants. However, disruption of both *ICS1/SID2* and *FMO1* abolished the enhanced immunity of the callose synthase mutants against the fungal pathogen. Therefore, while NHP plays a crucial role in the early senescence of *pmr4/gsl5* mutants, both SA and NHP have important roles in the strong powdery mildew resistance induced by the loss of the callose synthase.

Introduction

Plants have a sophisticated innate immune system that enables them to detect and defend against infection by pathogens (Jones and Dangl 2006; Li et al. 2020; Jones et al. 2024). Pathogen-associated molecular patterns (PAMPs), such as bacterial flagellin, can activate PAMP-triggered immunity (PTI) upon recognition by pattern-recognition receptors on the plant host (Boutrot and Zipfel 2017; Zhang et al. 2024). PTI involves a series of rapid defense responses, including burst of reactive oxygen species, activation of mitogen-activated protein kinases, callose deposition, and expression of defense genes (Boutrot and Zipfel 2017; Zhang et al. 2024). Pathogens can counteract PTI by delivering effectors to plant cells. However, some of these pathogen effectors are recognized by plant resistance (R) proteins, which activate effector-triggered immunity (ETI) (Li et al. 2020; Jones et al. 2024). ETI is often characterized by a rapid programed cell death or hypersensitive responses (Jones and Dangl 2006), as well as increased accumulation of defense signal molecules such as salicylic acid (SA) and *N*-hydroxypipecolic acid (NHP). These defense signal molecules accumulate not only in the infection sites but also in distant, uninfected tissues to establish systemic acquired resistance (SAR) (Hartmann and Zeier 2019; Huang et al. 2020; Shields et al. 2022).

Activation of PTI, ETI, SAR, and other defense mechanisms can often negatively impact plant growth and, therefore, is tightly regulated (Karasov et al. 2017; He et al. 2022). In the absence of pathogen infection, plant immunity is generally kept at minimal levels due to the inactive state of immune receptors and the action of negative regulators of plant immune responses. Gain-of-function mutations in plant immune receptors or loss-of-function mutations in negative immune regulators can lead to constitutive defense and enhanced disease resistance, resulting in autoimmune mutants (van Wersch et al. 2016; Freh et al. 2022). These constitutive defense mechanisms in the autoimmune mutants often incur fitness costs, such as stunted growth, lesion development, and early senescence (van Wersch et al. 2016; Zhang et al. 2020). The morphological phenotypes resulting from the mutations of plant immune receptors in autoimmune mutants have been utilized to analyze the structure-function relationship of these receptors, their biogenesis, and downstream signaling pathways (van Wersch et al. 2016; Freh et al. 2022). Additionally, the lesion-mimic and early senescence phenotypes of many autoimmune mutants have been used to investigate the components and pathways involved in these growth defects and the relationship with their autoimmunity (van Wersch et al. 2016; Zhang et al. 2020; Freh et al. 2022).

Received February 23, 2025. Accepted March 23, 2025.

One well-characterized defense mechanism in plants is the pathogen-induced deposition of callose, a β-(1,3)-D-glucan polymer also found in sieve plates, pollen tubes, microsporocytes, cell plates, and plasmodesmata (Ellinger and Voigt 2014; Wang et al. 2021). Callose polymers are thought to reinforce the cell wall structure at the infection sites, thereby restricting the ingression of pathogen-secreted cell wall-degrading enzymes (Stone and Clarke 1992). In Arabidopsis, pathogen-induced callose deposition is dependent on the POWDERY MILDEW RESISTANT 4/GLUCAN SYNTHASE-LIKE 5 (PMR4/GSL5) callose synthase (Jacobs et al. 2003; Nishimura et al. 2003). Arabidopsis *pmr4/gsl5* mutant plants are hypersusceptible to a strain of *Pseudomonas syringae* that lacks the type III secretion system, underscoring the critical role of pathogen-induced callose deposition in PTI (Kim et al. 2005). Overexpression of *PMR4* in transgenic Arabidopsis plants confers complete restriction of penetration by powdery mildew fungal pathogen (Ellinger et al. 2013), further highlighting the importance of callose deposition in plant immunity. We have shown that 2 Arabidopsis homologs of UBIQUITIN-ASSOCIATED DOMAIN-CONTAINING PROTEIN 2 (UBAC2), a conserved endoplasmic reticulum (ER) protein involved in ER protein quality control, interact with the plant-specific ER protein PAMP-INDUCED COILED COIL (PICC) to regulate PMR4/GSL5 production and play an important role in plant immunity (Wang et al. 2019). Mutants for both UBAC2s and PICC were compromised in PTI due to reduced accumulation of PMR4/GSL5 callose synthase and deficiency in pathogen-induced callose deposition (Wang et al. 2019).

Unexpectedly, mutations of *PMR4/GSL5* result in increased resistance to powdery mildew and downy mildew (Vogel and Somerville 2000; Jacobs et al. 2003; Nishimura et al. 2003). The enhanced powdery mildew resistance in *pmr4/gsl5* mutants was associated with elevated SA levels and increased expression of SA-responsive genes, including *PATHOGENESIS-RELATED* (*PR*) genes (Nishimura et al. 2003). Disruption of *PHYTOALEXIN DEFICIENT4* (*PAD4*), a key regulator of plant immunity that controls SA accumulation, or expression of the bacterial *nahG* gene, which encodes an SA hydroxylase, completely abolished the powdery mildew resistance of the *pmr4/gsl5* mutants (Nishimura et al. 2003). The findings indicated a critical role for upregulated SA signaling in the enhanced powdery mildew resistance of *pmr4* mutants (Nishimura et al. 2003). It has been proposed that PMR4/GSL5-mediated callose deposition suppresses other defense pathways through negative feedback to mitigate potential detrimental effects on plant fitness (Nishimura et al. 2003). Thus, PMR4/GSL5-mediated callose deposition and the PMR4/GSL5 protein have complex roles in plant immune systems.

In this study, we report that Arabidopsis *pmr4/gsl5* mutants not only displayed reduced growth as previously reported (Enns et al. 2005) but also developed symptoms of necrosis and early senescence. Similar negative effects on plant growth and fitness have been observed in other plant mutants with enhanced defense responses, often linked to increased SA signaling (van Wersch et al. 2016; Zhang et al. 2020; Freh et al. 2022). Arabidopsis autophagy mutants, for instance, display early senescence in a manner dependent on the primary SA receptor NONEXPRESSOR OF PR GENES 1 (NPR1) (Yoshimoto et al. 2009; Zhang et al. 2023). Disruption of Arabidopsis *MILDEW RESISTANCE LOCUS O2* (*MLO2*) genes, also known as *PMR2*, confers powdery mildew resistance as well and causes early senescence in a PAD4- and SA-dependent manner (Consonni et al. 2006). Our genetic suppressor analysis revealed that the early senescence observed in *pmr4/gsl5* mutants was suppressed by mutations in *PAD4* and the NHP biosynthetic genes, *ABERRANT GROWTH AND DEATH2-LIKE DEFENSE RESPONSE PROTEIN1* (*ALD1*) and *FLAVIN-DEPENDENT MONOXYGENASE1* (*FMO1*), but not by mutation in the SA biosynthetic gene *ISOCHORISMATE SYNTHASE1/SA-INDUCTION DIFFICIENT 2* (*ICS1/SID2*). These findings indicate a critical role of NHP in the growth defects of *pmr4/gsl5* mutants. Furthermore, while disruption of *PAD4* completely abolished the powdery mildew resistance in *pmr4/gsl4*, mutations of *SID2*, *ALD1*, or *FMO1* had only a minor effect. However, disruption of both *SID2* and *FMO1* eliminated the strong powdery mildew resistance of *pmr4/gsl5*, indicating important roles of both SA and NHP in the enhanced resistance of the mutants. The differential reliance of growth defects and enhanced immunity on NHP and SA in autoimmune mutants like *pmr4/gsl5* provides valuable insights into the intricate dynamics of plant immunity and the defense-growth tradeoff. These insights can help develop approaches to generate disease-resistant plants without compromising overall fitness.

Results

Mutations of *PMR4* caused necrosis and early senescence

We previously reported that 2 Arabidopsis homologs of UBAC2, a conserved ER protein involved in ER protein quality control, interact with the plant-specific ER protein PICC to regulate pathogen-induced callose deposition and PTI by promoting the accumulation of ER-synthesized PMR4/GSL5 callose synthase (Wang et al. 2019). In our study, we used 2 independent *pmr4/gsl5* mutants: *pmr4-1*, which contains a missense mutation that generates a stop codon at amino acid residue 687 (Nishimura et al. 2003), and *gsl5-1* (GABI_089H05), which contains a T-DNA insertion in the second exon of *PMR4/GSL5* (Jacobs et al. 2003). Under the growth conditions outlined in Materials and Methods section, *pmr4-1* and *gsl5-1* mutants grew normally during the first 4 to 5 wks postgermination, with sizes comparable to those of wild type (WT) (Fig. 1). However, starting from the 6th wk postgermination, the growth of the *pmr4-1* and *gsl5-1* mutants began to decline when compared with WT plants, as evidenced by their substantially reduced size (Fig. 1). Additionally, fully expanded leaves of *pmr4-1* and *gsl5-1* mutant plants, but not those of WT plants, started developing chlorotic and necrotic senescence symptoms (Fig. 1). By the 9th wk postgermination, a majority of fully expanded leaves of the *pmr4-1* and *gsl5-1* mutant plants exhibited these senescence symptoms, whereas WT leaves remained fully green (Fig. 1). Therefore, disruption of *PMR4/GSL5* not only enhances disease resistance but also leads to growth impairment and early senescence.

Early leaf senescence of *pmr4/gsl5* is dependent on *PAD4*

The *pmr4/gsl5* mutants exhibit strong resistance to both powdery and downy mildew (Vogel and Somerville 2000; Jacobs et al. 2003; Nishimura et al. 2003). The enhanced powdery mildew resistance in *pmr4* mutants was linked to upregulated SA signaling based on the dependance on *PAD4* and its abolishment by expressing the bacterial *nahG* SA hydroxylase gene (Nishimura et al. 2003). Increased SA signaling is known to promote both disease resistance and accelerate leaf senescence (Morris et al. 2000; Manacorda et al. 2013; Smith 2019; Zhang et al. 2021; Tan et al. 2024), and may contribute to the early senescence observed in *pmr4/gsl5* mutants. To investigate whether SA or another signaling pathway is responsible for the early senescence in *pmr4/gsl5* mutants, we mutagenized *gsl5-1* seeds with ethyl methanesulfonate

Figure 1. Growth defects and early senescence in the *pmr4/gsl5* mutants. Comparison of growth and morphology among WT, *pmr4-1*, and *gsl5-1* mutants at indicated weeks of age. Fully expanded rosette leaves of 9-wk-old WT and mutant plants are also shown. Scale bar: 1 cm.

(EMS) and isolated strong extragenic, recessive *suppressors of pmr4* (*spm*) from EMS-mutagenized *gsl5-1* plants at the M2 generation. Unlike the *gsl5* single mutant, these isolated *gsl5 spm* double mutants exhibited normal growth similar to WT, and their fully expanded leaves remained green at 8 to 9 wks postgermination. To identify the *spm* mutations, we employed bulked segregant analysis combined with next-generation sequencing (BSA-NGS). Linkage analysis of single nucleotide polymorphisms (SNPs) mapped the causal mutation of *spm1-1* to a region on the lower arm of chromosome III, which contains a mutation in *PAD4*. Specifically, *spm1-1* harbors a G-to-A substitution in the second exon at position 1,491 from the start codon of *PAD4*, resulting in a premature stop codon after amino acid residue 129 (Table 1; Fig. 2A).

To confirm that disruption of *PAD4* suppresses the early senescence phenotype of *pmr4/gsl5*, we examined the previously

Table 1. SPM genes and alleles

Gene name	Allele name	Nucleotide (nt) change	Amino acid (aa) change
SPM1/PAD4	*spm1-1*	G to A at nt 1491	Stop at aa 129
SPM2/ALD1	*spm2-1*	G deletion at nt 2,182	Frame shift after aa 119
	spm2-2	G to A at nt 332	Arg to Gln at aa 40
	spm2-3	G to A at nt 2952	Stop at aa 295
SPM3/FMO1	*spm3-1*	G to A at nt 1282	Stop at aa 256
	spm3-2	C to T at nt 875	Ala to Val at aa 220

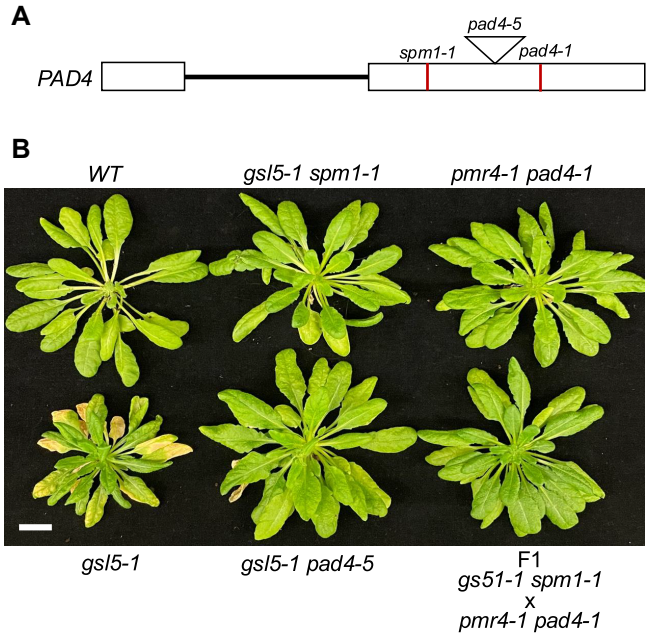

Figure 2. Disruption of *PAD4* suppressed early senescence in the *pmr4/gsl5* mutant. **A)** Structure of the *PAD4* gene and mutations in *pad4/spm1* mutants. The exons of *PAD4* are depicted as open boxes and introns are shown as lines. The locations of point mutations in *pad4-1* and *spm1-1*, as well as the T-DNA insertion site in *pad4-5* are indicated. **B)** Comparison of growth and morphology at 9-wks of age among WT, *gsl5-1* single mutant, *pmr4/gsl5*-containing double mutants, and the F1 hybrid from the cross between *gsl5-1 spm1-1* and *pmr4-1 pad4-1* for allelism test. Scale bar: 1 cm.

reported *pmr4-1 pad4-1* double mutant (Nishimura et al. 2003). This double mutant displayed normal growth without the early senescence phenotype characteristic of *pmr4-1* (Figs. 1 and 2). Additionally, we obtained a T-DNA knockout mutant for *PAD4* (*pad4-5*) (Fig. 2A) and generated the *gsl5-1 pad4-5* double mutant. The *pad4-5* mutation in the *gsl5-1 pad4-5* double mutant effectively suppressed both the growth defects and early senescence of *gsl5-1* (Fig. 2B). Furthermore, crossing the *pmr4-1 pad4-1* double mutant with *gsl5-1 spm1-1* double mutant resulted in F1 progeny that exhibited normal growth without early senescence (Fig. 2), indicating that *spm1-1* and *pad4-1* are allelic. These findings confirm that *PAD4* is crucial not only for enhanced powdery mildew resistance but also for the early senescence of the *pmr4/gsl5* mutants.

Early leaf senescence of *pmr4* is also dependent on *ALD1* and *FMO1*

Using the BSA-NGS approach, we mapped the causal mutations of *spm2-1* to the top arm of chromosome II, identifying a mutation in *ALD1*, an NHP biosynthetic gene. Specifically, *spm2-1* contains a G

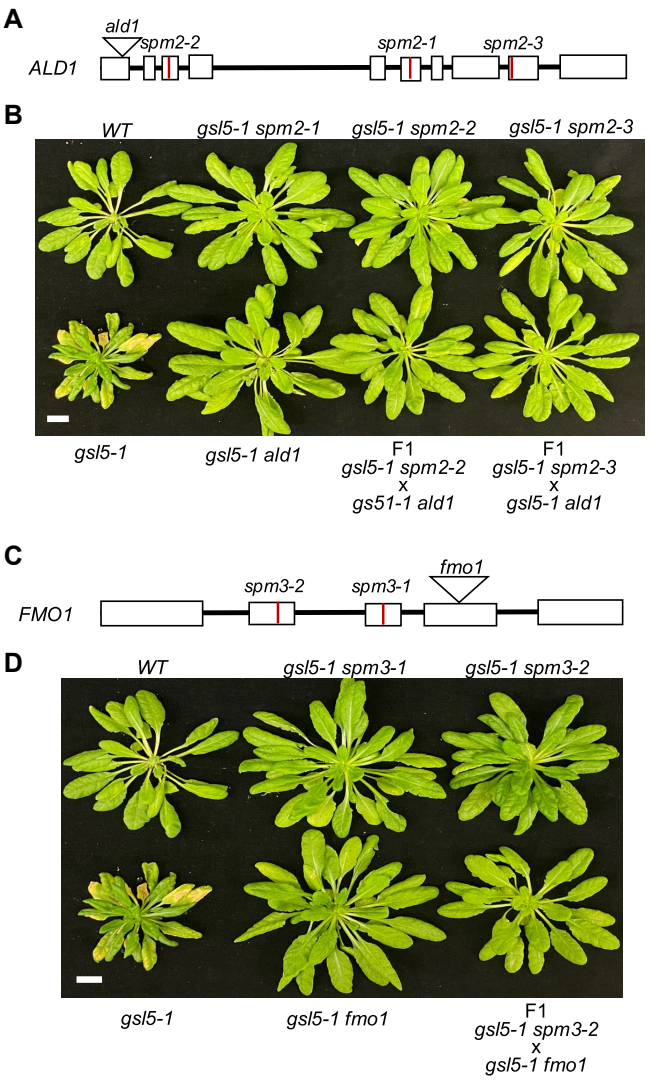

Figure 3. Disruption of NHP biosynthetic gene *ALD1* or *FMO1* suppressed early senescence in the *gsl5-1* mutant. **A)** Structure of the *ALD1* gene and mutations in *ald1/spm2* mutants. The exons of *ALD1* are depicted as open boxes and introns are shown as lines. The locations of point mutations in *spm2-1*, *spm2-2*, *spm2-3* and the T-DNA insertion site in *ald1* are indicated. **B)** Comparison of growth and morphology among 9-wks old WT, *gsl5-1* single mutant, *gsl5*-containing double mutants, and the F1 hybrid from the cross between *gsl5-1 spm2-2*×*gsl5-1 ald1*, and between *gsl5-1 spm2-3* and *gsl5-1 ald1* for allelism test. Scale bar: 1 cm. **C)** Structure of the *FMO1* gene and mutations in *fmo1/spm3* mutants. The exons of *FMO1* are shown as open boxes and introns are depicted as lines. The locations of point mutations in *spm3-1*, *spm3-2*, and the T-DNA insertion site in *fmo1* are indicated. **D)** Comparison of growth and morphology among 9-wks old WT, *gsl5-1* single mutant, *gsl5*-containing double mutants, and the F1 hybrid from the cross between *gsl5-1 spm3-2*×*gsl5-1 fmo1* for allelism test. Scale bar: 1 cm. The WT and mutant plants in Figs. 2B, 3, B and D, and 4B were grown concurrently under identical conditions. The same images of WT and *gsl5-1* mutant plants were used across these figures for consistency.

deletion in the 6th exon at position 2,182 from the start codon of the *ALD1* gene, which introduces a frameshift in translation after the first 119 amino acid residues (Table 1; Fig. 3A). To confirm that disruption of *ALD1* suppresses the early leaf senescence of *gsl5*, we obtained an *ald1* T-DNA insertion mutant (Fig. 3A) and created the *gsl5-1 ald1* double mutant through genetic crossing. As shown in Fig. 3B, the *ald1* mutation in the double mutant completely suppressed the growth defects and early senescence phenotypes of *gsl5-1*. Allelism tests identified 2 additional *spm2* mutants (*spm2-2* and *2-3*), both with mutations in *ALD1* (Fig. 3, A and B). The mutation in *spm2-2* is a G-to-A substitution in the third exon at position 332 from the start codon of the *ALD1* gene, altering a highly conserved arginine residue to glutamine at amino acid position 40 (Table 1; Fig. 3A). The *spm2-3* mutation is also a G-to-A substitution in the 9th exon at position 2,952 from the start codon, leading to a premature stop codon after amino acid residue 295 (Table 1; Fig. 3A). These results indicate that the NHP biosynthetic gene *ALD1* is required for the early senescence of *pmr4/gsl5* mutants.

The causal mutation of *spm3-1* was mapped to a region on chromosome I through BSA-NGS, where we identified a mutation in *FMO1*, another NHP biosynthetic gene (Fig. 3C). The *spm3-1* mutation is a G-to-A substitution in the 3rd exon at position 1,282 from the start codon of the *FMO1* gene, introducing a premature stop codon after amino acid residue 256. Additionally, *spm3-2* carries a C-to-T substitution in the 2nd exon at position 875 from the start codon, changing a highly conserved alanine residue to valine at amino acid position 220 (Table 1; Fig. 3C). To confirm that disruption of *FMO1* suppresses early senescence of *gsl5-1*, we obtained a *fmo1* T-DNA insertion mutant and generated the *gsl5-1 fmo1* double mutant (Fig. 3C). As shown in Fig. 3D, T-DNA disruption of *FMO1* in the *gsl5-1 fmo1* double mutant fully suppressed the growth defects and early senescence of *gsl5-1*. We also crossed *gsl5-1 spm3-2* with *gsl5-1 fmo1* and found that the resulting F1 progeny all resembled their parental plants with normal growth and no early senescence (Fig. 3D). These findings confirm that the early senescence of *pmr4/gsl5* mutants is dependent on *FMO1*.

Early leaf senescence of *pmr4* is independent of *ICS1/SID2*

The enhanced powdery mildew resistance in the *pmr4/gsl5* mutants has been attributed to upregulated SA signaling because it was dependent on PAD4, which regulates SA accumulation, and was suppressed by expressing bacterial NahG SA hydroxylase (Nishimura et al. 2003). Despite this association with SA signaling, none of the isolated *spm* mutants were from mutations in SA biosynthetic or signaling genes. To investigate the role of SA in the early senescence observed in *pmr4/gsl5*, we crossed the *gsl5-1* mutant with a T-DNA knockout mutant for *ICS1/SID2*, which encodes a key enzyme for pathogen- and stress-induced SA production (Fig. 4A). The resulting *gsl5-1 sid2* double mutant was compared with WT and the *gsl5-1* single mutant. As shown in Fig. 4B, unlike the *gsl5-1 pad4*, *gsl5-1 ald1* and *gsl5-1 fmo1* double mutants (Figs. 2 and 3), the *gsl5-1 sid2* double mutant displayed early senescence similar to that of the *gsl5-1* single mutant (Fig. 4B). This indicates that early senescence in *pmr4/gsl5* is not dependent on SA biosynthetic gene *ICS1/SID2*.

Association between pipecolic acid accumulation and early senescence in WT and mutants

To further investigate the role of NHP in the early senescence of *pmr4/gsl5*, we analyzed the levels of pipecolic acid in WT and mutant plants. Pipecolic acid, the precursor to NHP, and NHP itself both increase in response to immune activation (Chen et al. 2018; Hartmann et al. 2018; Wang et al. 2018; Brambilla et al. 2023). While pipecolic acid is detectable even in uninfected Arabidopsis plants, NHP is usually present at very low levels in uninfected plants, often below the detection limit of gas chromatography/mass spectrometry (GC/MS)-based methods (Chen et al. 2018; Wang et al. 2018; Holmes et al. 2021). We analyzed the levels of pipecolic acid in the leaves of 5- and 9-wk-old WT, as well as

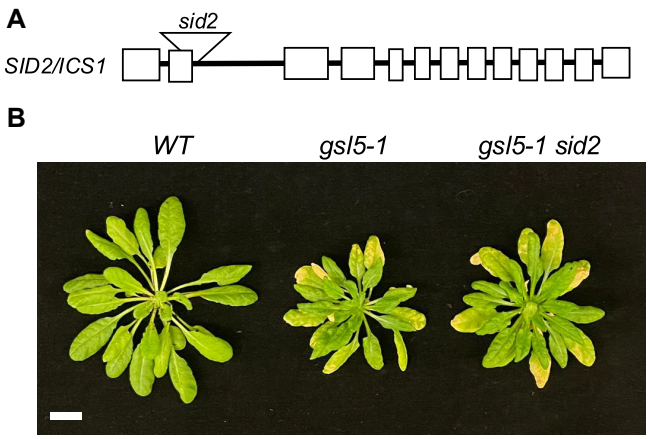

Figure 4. Disruption of SA biosynthetic gene *SID2* failed to suppress early senescence of *gsl5-1* mutant. **A)** Structure of the *SID2/ICS1* gene and mutation in *sid2* mutant. The exons of *SID2/ICS1* are depicted as open boxes and introns are shown as lines. The location of the T-DNA insertion site in *sid2* is indicated. **B)** Comparison of growth and morphology among 9-wks old WT, *gsl5-1* single mutant, and *gsl5 sid2* double mutants. Scale bar: 1 cm. The WT and mutant plants in Figs. 2B, 3B, 3D, and 4B were grown concurrently under identical conditions. The same images of WT and *gsl5-1* mutant plants were used across these figures for consistency.

pmr4/gsl5 single and various *pmr4/gsl5*-containing double mutants. At 5 wks of age, *pmr4-1* and *gsl5-1* mutants exhibited no visible senescence symptoms and were morphologically indistinguishable from WT plants. However, the levels of pipecolic acid in both *pmr4-1* and *gsl5-1* mutants were more than 200-fold higher than in WT (Fig. 5A). The elevated levels of pipecolic acid in the *pmr4/gsl5* single mutants were completely suppressed by the mutations in *PAD4* and *ALD1*, as observed in the *pmr4-1 pad4* and *gsl5-1 ald1* double mutants, respectively (Fig. 5A). Interestingly, the loss of FMO1, which catalyzes the conversion of pipecolic acid to NHP, also greatly reduced the levels of pipecolic acid in the *gsl5-1 fmo1* double mutant, which were about 50-fold lower than in the *gsl5-1* single mutant but about 6-fold higher than in WT (Fig. 5A). In contrast, disruption of *SID2* did not substantially reduce pipecolic acid accumulation in the *gsl5-1 sid2* double mutant, whose pipecolic acid levels were still over 160-fold higher than those in WT (Fig. 5A). Thus, early senescence was strongly associated with strong pipecolic acid accumulation, highlighting a critical role for pipecolic acid accumulation in the observed phenotypes.

At 9 wks, *pmr4/gsl5* mutants already displayed the senescence symptoms of chlorosis and necrosis, whereas WT plants did not (Fig. 1). The levels of pipecolic acid in the *pmr4/gsl5* mutants were ~20-fold higher than those in WT at this age (Fig. 5B). Although this represented a substantial increase, it was lower compared with the over 200-fold elevation at 5 wks of age (Fig. 5A). Again, disruption of *PAD4* or *ALD1* reduced pipecolic acid levels to below those in WT (Fig. 5B). Additionally, the levels of pipecolic acid in the *gsl5-1 fmo1* double mutant were substantially lower than those in the *gsl5* single mutant (Fig. 5B). This reduction of pipecolic acid levels in the *gsl5-1 fmo1* double mutant suggests that FMO1, which converts pipecolic acid to NHP, may regulates pipecolic acid accumulation through a positive feedback mechanism. As seen at 5 wks, the levels of pipecolic acid in the *gsl1-1 sid2* double mutant were comparable to those in the *gsl5-1* single mutant at 9 wks (Fig. 5B). Therefore, disruption of *SID2* had no effect on the high accumulation of pipecolic acid in *gsl5* mutants at either age.

Lack of association between SA accumulation and early senescence in WT and mutants

We also compared the levels of free SA and the combined free SA and SA glucoside (SA + SAG) in the leaves of 5- and 9-wk-old WT and *pmr4/gsl5* single, as well as various *pmr4/gsl5*-containing double mutants. At 5 wks, while pipecolic acid levels in the *pmr4/gsl5* mutants increased over 200-fold, both SA and SA + SAG levels in the mutants were only about 100–150% higher than in WT (Fig. 6A). Notably, SA and SA + SAG levels in the *pmr4-1 pad4* double mutant were about 3- to 6-fold lower than in WT (Fig. 6A), indicating a crucial role of PAD4 in the elevated basal levels of SA in the *pmr4/gsl5* mutants. As expected, SA and SA + SAG levels in the *pmr4-1 sid2* double mutant were similar to those in the *pmr4-1 pad4* double mutant and were also about 3- to 6-fold lower than in WT (Fig. 6A). On the other hand, the levels of SA and SA + SAG in the *gsl5-1 ald1* and *gsl5-1 fmo1* were similar to, but not lower than, those in WT (Fig. 6A). Thus, while the disruption of NHP biosynthetic genes *ALD1* and *FMO1* did not reduce SA levels below WT levels, it could suppress the significant increase in SA levels in *pmr4/gsl5* mutants at the growth stage prior to senescence.

At 9 wks, the *pmr4/gsl5* mutants already developed extensive senescence symptoms (Fig. 1), and their SA and SA + SAG levels were further elevated to ~10 times those in WT (Fig. 6B). Disruption of *PAD4* again reduced both SA and SA + SAG levels in the *gsl1 pad4* double mutants substantially below those in WT (Fig. 6B). Mutations of *ALD1* or *FMO1* in their respective double mutants with *gsl5-1* also completely suppressed the elevated SA and SA + SAG levels caused by the disruption of *PMR4/GSL5* (Fig. 6B). The suppression of SA and SA + SAG accumulation in the *pmr4 pad4*, *gsl5 ald1* and *gsl5 fmo1* double mutants was associated with the complete suppression of the early senescence phenotype seen in the *pmr4/gsl5* single mutants (Figs. 2 and 3). On the other hand, disruption of *SID2* in the *gsl1 sid2* double mutants also completely suppressed the greatly elevated SA and SA + SAG levels seen in the *gsl5* single mutant (Fig. 6B), but both the *gsl5-1* single and *gsl5-1 sid2* double mutants developed extensive senescence symptoms at the same growth stage (Fig. 4). Thus, early senescence of these mutants was associated only with the accumulation of pipecolic acid but not with the accumulation of SA.

Role of PAD4, SA, NHP, and NPR1 in *pmr4/gsl5* powdery mildew resistance

To explore the relationship of early senescence with enhanced disease resistance due to the loss of PMR4 callose synthase, we examined how mutations in *PAD4*, *ALD1*, *FMO1*, and *SID2* affect the powdery mildew resistance in the *pmr4/gsl5* mutants. After inoculation with the adapted powdery mildew isolate *Golovinomyces cichoracearum* UCSC1, we confirmed that both *pmr4-1* and *gsl5-1* mutants were highly resistant to the fungal pathogen (Supplementary Fig. S1). Unlike WT, *pad4*, *ald1*, *fmo1*, and *sid2* mutant plants, which were all highly susceptible to powdery mildew, as evidenced by extensive whitish powdery mildew (Supplementary Fig. S1A) and a high number of fungal spore (conidia) counts (Supplementary Fig. S1B) at 10 d postinoculation (dpi), both *pmr4-1* and *gsl5-1* mutants displayed minimal whitish mildew symptoms on leaf surface (Supplementary Fig. S1A) and a 10- to 20-fold reduction in fungal sporulation compared with WT and the mutants (Supplementary Fig. S1B). The strong powdery mildew resistance in *gsl5-1* was completely suppressed in the *gsl5-1 pad4* double mutant, as shown by both symptom development and sporulation (Fig. 7), confirming the critical role of

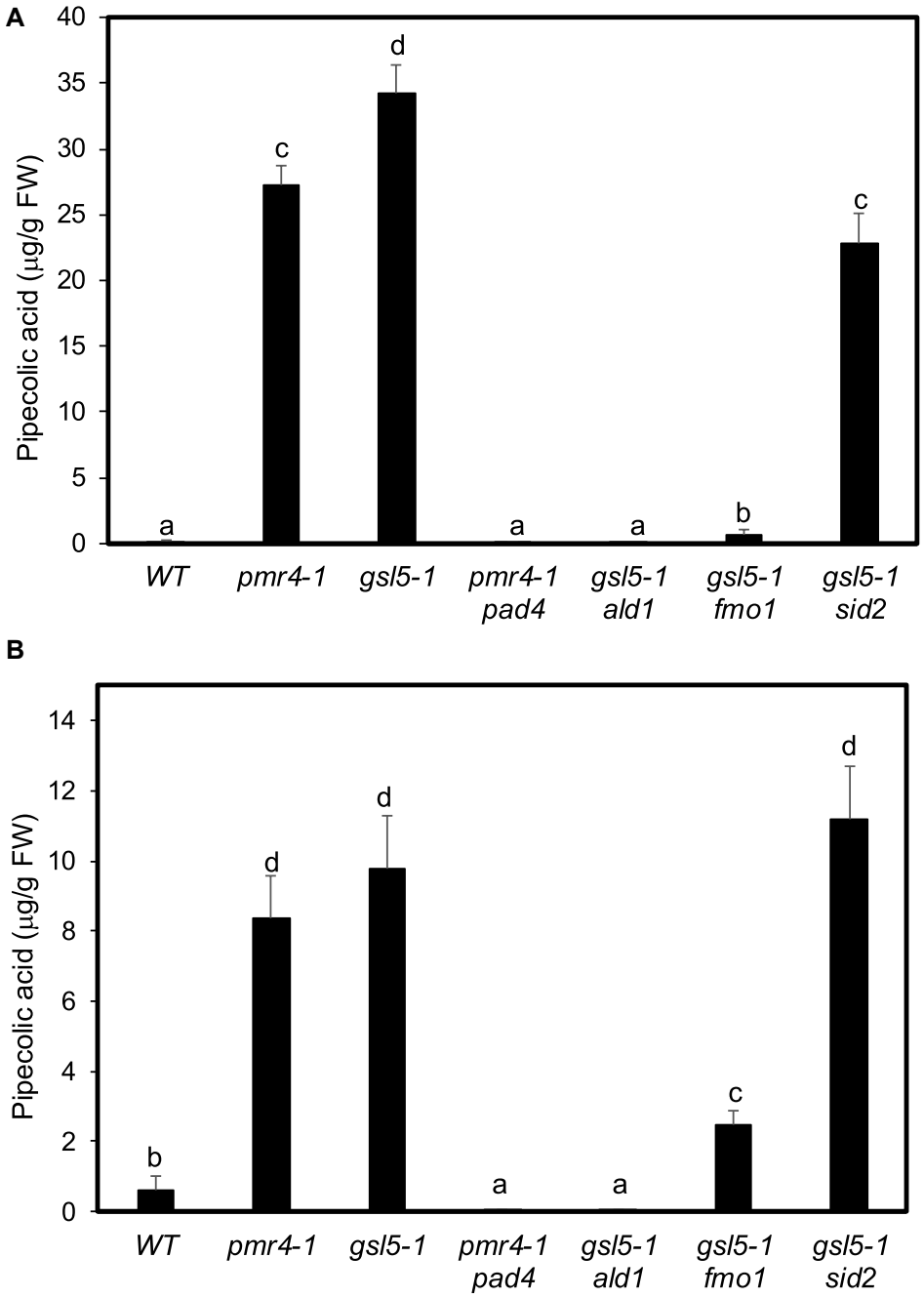

Figure 5. Accumulation of pipecolic acid in WT and mutants. Pipecolic acid contents in **A)** 5-wk-, and **B)** 9-wk-old WT, *pmr4/gsl5* single mutants, and *pmr4/gsl5*-containing double mutant plants. Means and standard errors were calculated from average pipecolic acid contents determined from 3 samples for each genotype. According to Duncan's multiple range test ($P = 0.01$), means of pipecolic acid contents differ significantly if they are indicated with different letters.

PAD4 in the powdery mildew resistance of the *pmr4/gsl5* mutants (Nishimura et al. 2003). Expression of *nahG* SA hydroxylase gene in *pmr4-1* also completely abolished the strong powdery mildew resistance of the *pmr4-1* mutant, based on both the symptom development and sporulation (Fig. 7). In contrast, the symptom development and sporulation of the *gsl1-1 npr1* double mutant were only slightly elevated when compared with those of the *gsl5-1* single mutant (Fig. 7). Thus, the effects of *pad4* and *npr1* mutations, as well as *nahG* expression, on the powdery mildew resistance of the *pmr4/gsl5* mutants were highly consistent with previous findings (Nishimura et al. 2003).

Interestingly, both the *gsl5-1 ald1* and *gsl5-1 fmo1* double mutants, which are normal in growth, remained highly resistant to the powdery mildew fungal pathogen, with only minor whitish symptoms (Fig. 7A) and low levels of sporulation (Fig. 7B). Sporulation of the fungal pathogen on the leaves of *gsl1-1 ald1* and *gsl1-1 fmo1* double mutants was increased by about 2- to 3-fold from those of the *gsl5-1* single mutant, but remained about 5-fold lower than in WT (Fig. 7B). Thus, while the *ald1* and *fmo1* mutations completely suppressed the growth defects and early senescence of *pmr4/gsl5* mutants (Fig. 3), they had only a minor effect on powdery mildew resistance (Fig. 7). Disruption of *SID2* also

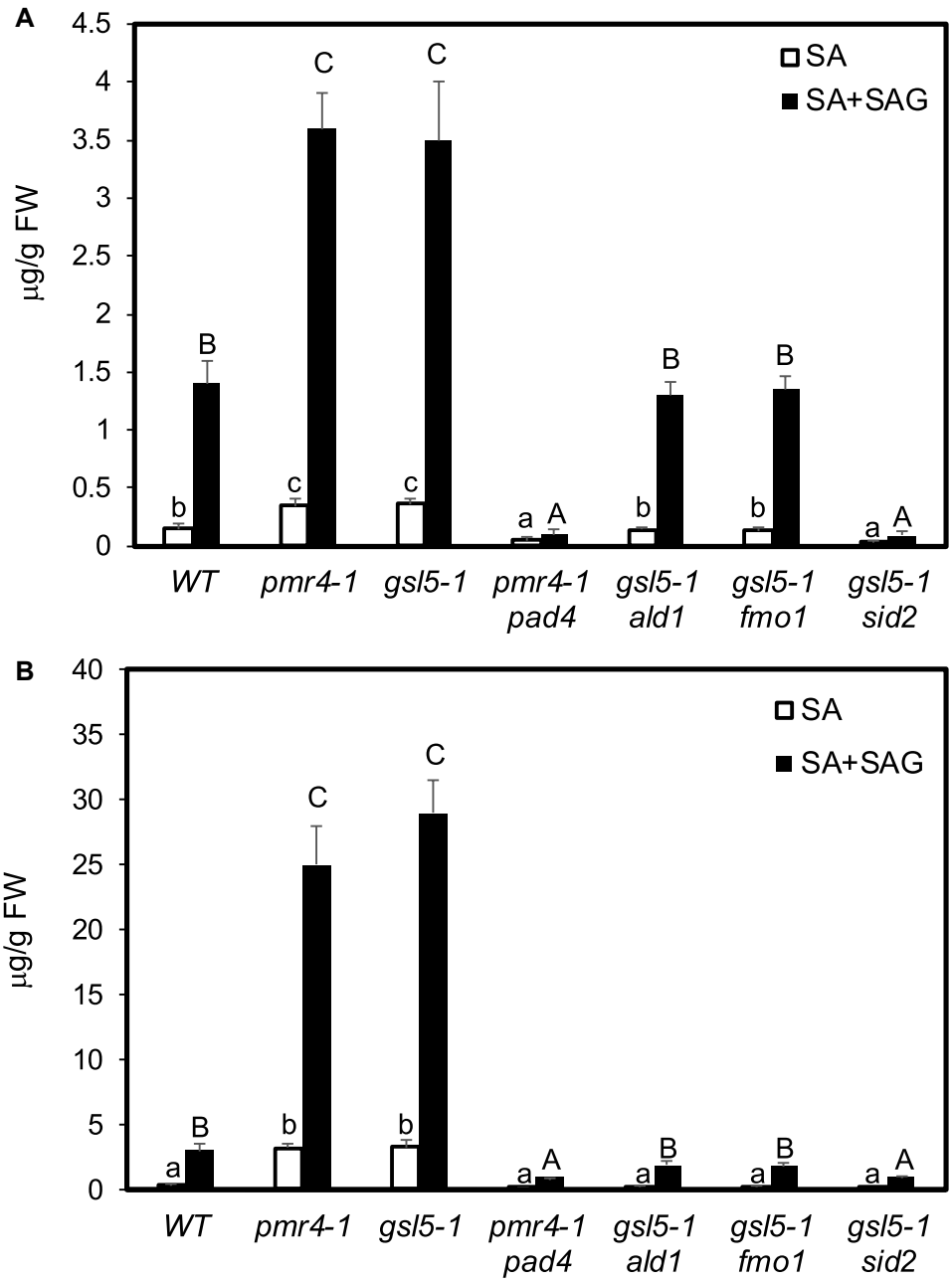

Figure 6. Accumulation of SA in WT and mutants. SA and SA + SAG contents in **A)** 5-wk-, and **B)** 9-wk-old WT, *pmr4/gsl5* single mutants, and *pmr4/gsl5*-containing double mutant plants. Means and standard errors were calculated from average SA contents determined from 3 samples for each genotype. According to Duncan's multiple range test ($P = 0.01$), means differ significantly if they are indicated with different lowercase letters for free SA and with different uppercase letters for SA + SAG.

had little effect on the powdery mildew resistance in the *sid2 gsl5-1* double mutant, despite the previously documented role of SA (Fig. 7). This SA-deficient double mutant displayed similar levels of powdery mildew resistance as *gsl5-1 ald1* and *gsl5-1 fmo1* double mutants, with very limited whitish symptoms (Fig. 7A) and low levels of sporulation (Fig. 7B). Therefore, disruption of *SID2* did not substantially affect either the early senescence or the powdery mildew resistance of *pmr4/gsl5* mutants.

Considering the coordinated and additive roles of SA and NHP in plant immunity (Hartmann and Zeier 2019; Yildiz et al. 2021; Shields et al. 2022; Lim 2023), we also generated a *gsl1-5 fmo1 sid2* triple mutant to explore the combined effects of disrupting both *SID2* and *FMO1* on the powdery mildew resistance triggered by the loss of the PMR4/GSL5 callose synthase. Importantly, loss of both SID2 and FMO1 completely suppressed the strong powdery mildew resistance conferred by the loss of the PMR4/GSL5 callose synthase, as evidenced from the highly susceptible phenotype of the *gsl5-1 sid2 fmo1* triple mutant based on its strong whitish powdery mildew symptoms and greatly elevated levels of sporulation (Fig. 7).

Basal and pathogen-induced PR1 gene expression

Given the differential effects of *nahG* expression, as well as the *pad4*, *npr1*, *sid2*, *ald1*, *fmol1* single, and *sid2 fmo1* double mutations on the *pmr4/gsl5* powdery mildew resistance, we performed

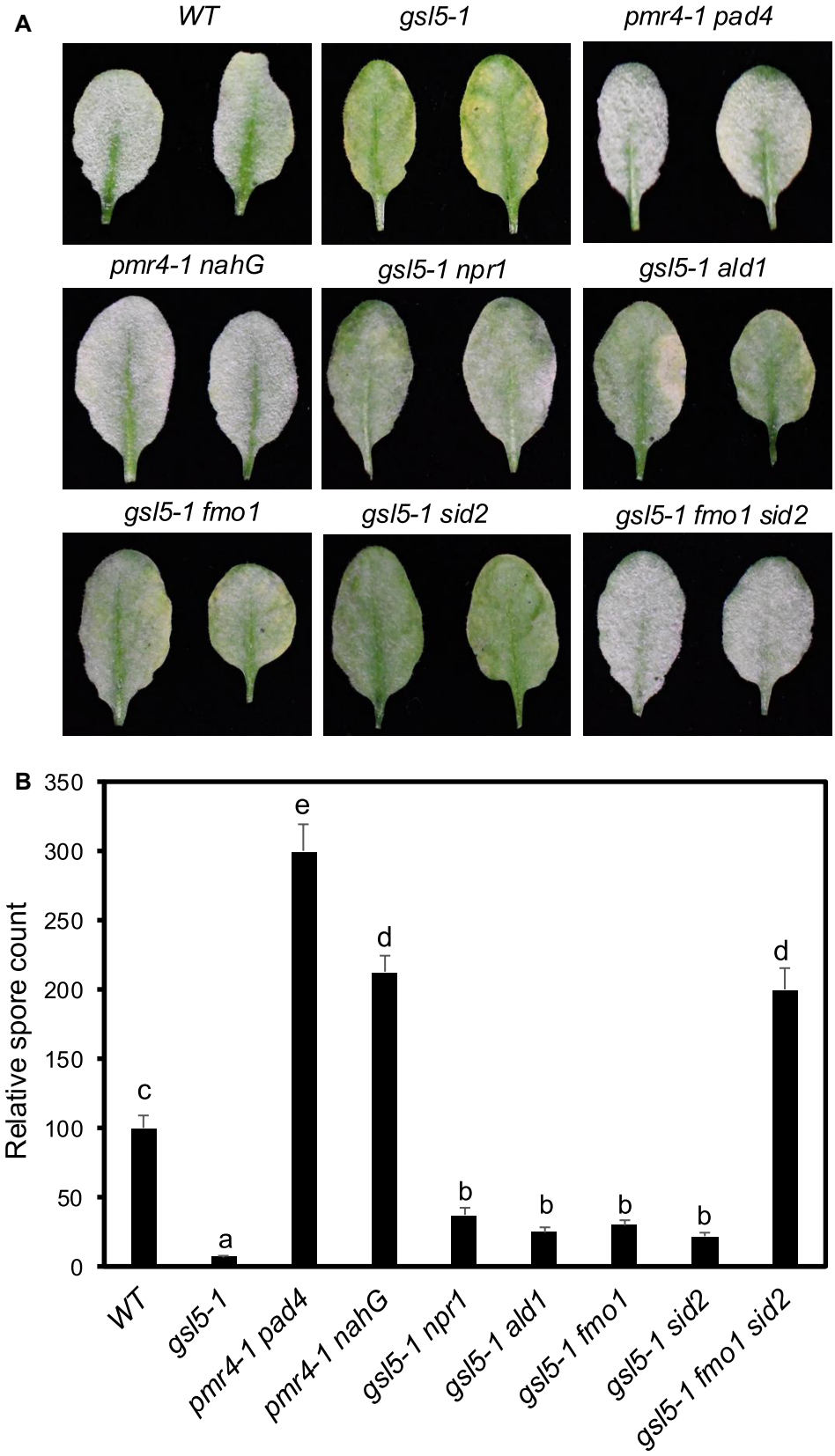

Figure 7. Effects of *pad4*, *npr1*, *ald1*, *fmo1*, *sid2* single mutations, *nahG* expression, and *sid2 fmo1* double mutations on the powdery mildew resistance of *pmr4/gsl5* mutants. **A)** Disease symptoms of fully expanded leaves of WT and mutant plants at 10 dpi. **B)** Relative spore counts on fully expanded leaves of WT and mutant plants at 10 dpi. Spore numbers/mg fresh leaf weight of mutants were normalized to WT for calculation of relative spore counts. Means and standard errors were calculated from average spore numbers determined from 6 samples for each genotype. According to Duncan's multiple range test ($P = 0.01$), means of spore numbers differ significantly if they are indicated with different letters. The experiments were repeated twice with similar results.

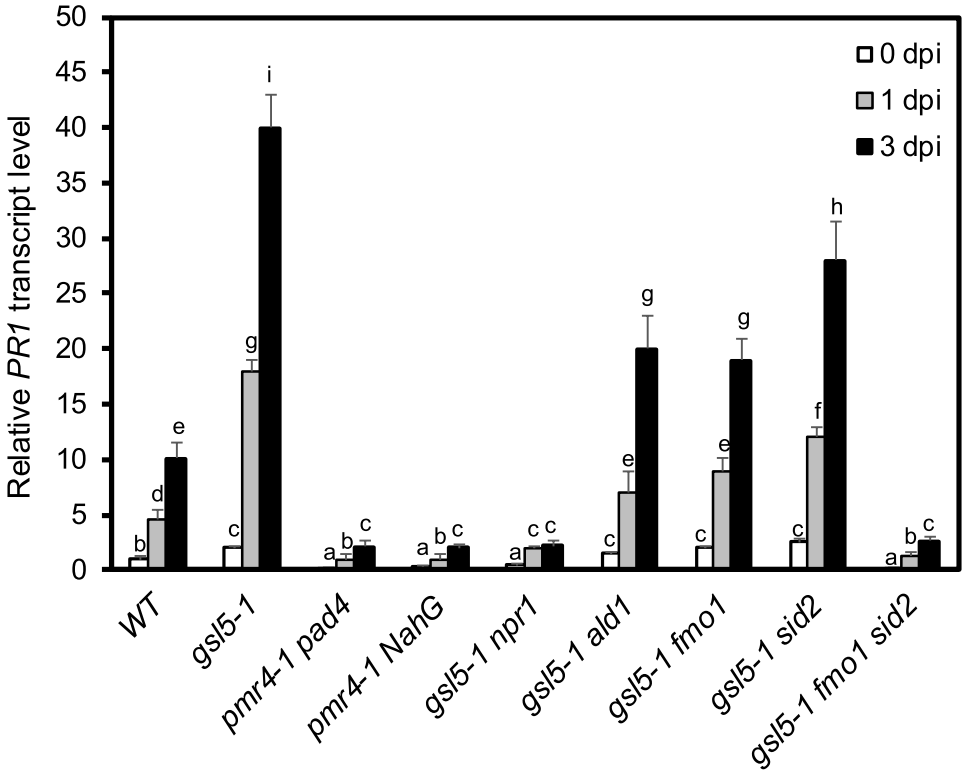

Figure 8. Effects of *pad4*, *npr1*, *ald1*, *fmo1*, *sid2* single mutation, *nahG* expression, and *sid2 fmo1* double mutations on basal and pathogen-induced *PR1* gene expression in *pmr4/gsl5* mutants. Five-week-old WT and mutant plants were inoculated with the adapted powdery mildew fungal pathogen and leaf tissues were harvested at 0, 1, and 3 dpi for RNA isolation. Relative *PR1* transcript levels were determined by RT-qPCR using gene-specific primers. Means and standard errors were calculated from 3 replicates. According to Duncan's multiple range test ($P = 0.01$), means of relative *PR1* transcript levels differ significantly if they are indicated with different letters.

reverse transcription quantitative PCR (RT-qPCR) to analyze their imparts on both basal and pathogen-induced expression of *PR1*, a defense marker gene associated with SA- and NHP-dependent SAR. In WT, the transcript levels of *PR1* increased about 5- and 10-fold at 1 and 3 dpi, respectively, when compared with the levels at 0 dpi (Fig. 8). In 5-wk-old *pmr4/gsl5* mutants, the levels of *PR1* transcripts were more than 2 times higher at 0 dpi, and about 4 times higher at both 1 and 3 dpi than the levels in WT (Fig. 8). The elevated basal and pathogen-induced *PR1* gene expression in the *gsl5* mutant plants was completely suppressed by *nahG* expression, the *pad4* and *npr1* single mutations, and the *sid2 fmo1* double mutations (Fig. 8). In contrast, the elevated basal and pathogen-induced *PR1* gene expression in the *gsl5* mutant plants was only partially suppressed by the *sid2*, *ald1* and *fmo1* single mutations (Fig. 8).

Discussion

Despite its critical role in pathogen-induced callose deposition and PTI, loss of PMR4/GSL5 callose synthase paradoxically leads to enhanced powdery mildew resistance, which was attributed to upregulated SA signaling (Nishimura et al. 2003). In this study, we further investigated the mutants for the PMR4/GSL5 callose synthase, uncovering important insights into the molecular mechanisms underlying their autoimmunity. Previously, Arabidopsis *pmr4/gsl5* mutants were reported to exhibit epinasty, particularly under short-day conditions (Vogel and Somerville 2000), and significant growth reduction (Enns et al. 2005). Silencing or knockout of a tomato *PMR4* homolog also resulted in significant growth reduction (Huibers et al. 2013; Santillan Martinez et al. 2020; Li et al. 2022). Under our growth conditions, however, Arabidopsis *pmr4/gsl5* mutants displayed even more severe growth impairment than previously described (Fig. 1). While these mutants grew normally for the first 4 to 5 wks after germination, they subsequently exhibited not only reduced growth but also additional phenotypes including necrosis and early senescence (Fig. 1). These findings indicate that the heightened defense responses and disease resistance observed in the *pmr4/gsl5* mutants may be associated with age-dependent growth defects and spontaneous cell death. These traits are reminiscent of phenotypes observed in other autoimmune mutants (van Wersch et al. 2016). The strong cell death and early senescence phenotypes in *pmr4/gsl5* mutants provide a powerful genetic system for dissecting the signaling pathways that drive the autoimmunity, which can offer a better understanding of the molecular basis of plant immunity and the tradeoff between defense and growth.

Despite the previously reported role of SA in the autoimmunity of the mutants, our genetic analysis revealed that disruption of SA biosynthetic gene *ICS1/SID2* had little effect on the growth defects of the *pmr4/gsl5* mutant plants (Fig. 4). In contrast the necrosis and early senescence phenotypes of *pmr4/gsl5* mutants were fully suppressed by the mutations of the NHP biosynthetic genes *ALD1* and *FMO1* (Fig. 3). Additional observations on the kinetics of pipecolic acid and SA accumulation, as well as their mutual regulation, further indicated that NHP, rather than SA, is the determining factor for the development of these growth phenotypes. At 5 wks of age, prior to the onset of growth phenotypes, there was already a drastic increase in pipecolic acid but only a very modest rise in SA in

the *pmr4/gsl5* mutants (Figs. 5 and 6). By 9 wks, when the senescence phenotypes were fully developed in the *pmr4/gsl5* mutants, the levels of pipecolic acid had decreased while SA levels increased when compared with those at 5 wks (Figs. 5 and 6). These patterns of pipecolic acid and SA accumulation suggest that increased levels of pipecolic acid, and consequently NHP, are the cause, while elevated SA levels are a secondary effect, of the growth defects and early senescence observed in the *pmr4/gsl5* mutants (Fig. 9). Disruption of *SID2*, which failed to suppress the early senescence (Fig. 4), had little effect on the drastic accumulation of pipecolic acid in the *gsl5-1 sid2* double mutant at both 5 and 9 wks of age (Fig. 5). In contrast, disruption *ALD1* and *FMO1* in the *gsl5-1 ald1* and *gsl5-1 fmo1* double mutants, respectively, suppressed both their early senescence and SA accumulation (Figs. 3 and 6). Thus, *pmr4/gsl5*-induced pipecolic acid accumulation is ICS1/SID2-independent and plays a crucial role in the growth defects of the mutant plants (Fig. 9). Similarly, in both Toll-like immune receptor-mediated defense activation, cell death and basal resistance, the role of NHP biosynthetic gene *FMO1* and its expression was independent of ICS1/SID2-dependent SA accumulation (Bartsch et al. 2006). These results are notable given the extensive coordination and mutual potentiation between SA and NHP in their biosynthesis, metabolism, and signaling (Hartmann and Zeier 2019; Huang et al. 2020; Shields et al. 2022).

Genetic analysis of the roles of SA and NHP biosynthetic genes in *pmr4/gsl5*-conferred powdery mildew resistance and defense-related *PR1* gene expression offered additional insights into the interplay among these defense regulatory factors in plant immunity. Similar to its effect on the growth defects, disruption of *ICS1/SID2* had only minor impact on the powdery mildew resistance of *pmr4/gsl5* mutant plants (Figs. 7). Likewise, mutations of *ALD1* or *FMO1* had a very limited effect on the powdery mildew resistance in *pmr4/gsl5* mutant plants (Figs. 7), despite their strong impact on the early senescence and associated growth defects (Fig. 3). These differential effects of the *ald1* and *fmo1* mutations indicated that the enhanced resistance and the associated growth defects in *pmr4/gsl5* mutants are only partially linked and can be largely uncoupled. The relative minor effect of the *sid2*, *ald1*, and *fmo1* mutations on the powdery mildew resistance in the *pmr4/gsl5* mutants was apparently caused by the redundant role of SA and NHP as disruption of both *SID2* and *FMO1* eliminated the powdery mildew resistance in the mutant plants (Fig. 7). Thus, while suppression of the growth defects of the *pmr4/gsl5* mutants requires only blocking NHP biosynthesis, suppression of the enhanced powdery mildew resistance necessitates blocking biosynthesis of both NHP and SA (Fig. 9). Pathogen-induced *PR1* expression was also only partially suppressed by the *sid2*, *ald1* or *fmo1* mutations, but was greatly reduced by mutations of both *SID2* and *FMO1* in the *pmr4/gsl5* mutant plants (Fig. 8), further indicating redundant roles of SA and NHP in the enhanced immunity of *pmr4/gsl5* mutant plants (Fig. 9). The *pmr4/gsl5* mutants contain highly elevated basal levels of pipecolic acid, as well as substantially elevated basal levels of SA (Figs. 5 and 6). The redundant roles of SA and NHP in the enhanced powdery mildew resistance of *pmr4/gsl5* mutants may be attributed to their relatively high levels, enabling them to mediate similar defense responses and defense gene expression in a largely independent manner. Similarly, both SA and NHP are strongly induced locally after infection by virulent or avirulent *Pseudomonas syringae*, and pathogen-induced *PR* gene expression at infection sites is also only partially reduced by mutations in *SID2*, *ALD1*, or *FMO1* (Zhou et al. 1998; Zheng et al. 2009; Navarova et al. 2012; Hartmann et al. 2018; Nair et al. 2021; Brambilla et al. 2023; Löwe et al. 2023). Analyses of *ald1 sid2* double mutants further support additive contributions of SA and NHP to basal immunity against *P. syringae* in Arabidopsis (Bernsdorff et al. 2016; Löwe et al. 2023).

Our analysis showed that the powdery mildew resistance of the *pmr4/gsl5* mutants was completely suppressed by the *pad4* mutation or the expression of *nahG*, but only marginally reduced by the *npr1* mutation (Fig. 7). These results closely aligned with those from the previous report, which served as key evidence supporting the critical role of SA signaling in the enhanced immunity of *pmr4/gsl5* mutants (Nishimura et al. 2003). These results are also consistent with the demonstrated overlapping roles of SA and NHP in the powdery mildew resistance of *pmr4/gsl5* mutants (Fig. 9). PAD4 plays a critical role not only in SA-regulated defense (Zhou et al. 1998; Jirage et al. 1999), but also in NHP accumulation(Cui et al. 2017; Joglekar et al. 2018; Hartmann and Zeier 2019; Huang et al. 2020; Dongus and Parker 2021; Feehan et al. 2023). Therefore, disruption of *PAD4* will block both SA- and NHP-induced defense, thereby compromising the enhanced immunity of the *pmr4/gsl5* mutants (Fig. 9). Similarly, the expression of bacterial *nahG* gene reduces not only ICS1/SID2-dependent inducible SA accumulation but also ICS2-dependent basal SA production, which is required for NHP-induced transcription (Nair et al. 2021). Expression of *nahG* is also known to alter SA-independent immune responses, including camalexin biosynthesis, and results in greater susceptibility to various pathogens than SA biosynthetic mutants (Nawrath and Metraux 1999; Heck et al. 2003; van Wees and Glazebrook 2003). On the other hand, NPR1 has been shown to be important for both SA-induced and NHP-induced defense transcription (Yildiz et al. 2021; Zavaliev and Dong 2024). Therefore, it would be expected to play a critical role in the SA- and NHP-dependent powdery mildew resistance of *pmr4/gsl5* mutants. However, disruption *NPR1* had only a minor effect on the powdery mildew resistance of *pmr4/gsl5* mutants (Nishimura et al. 2003) (Fig. 7). The limited role of NPR1 can be interpreted as the overlapping roles of SA and NHP in the *pmr4* powdery mildew resistance being mediated by both NPR1-dependent and NPR1-independent pathways (Nishimura et al. 2003).

The complete suppression of growth defects in the *pmr4/gsl5* mutants through disruption of NHP biosynthetic genes (Fig. 3), without substantially impacting their powdery mildew resistance (Figs. 7), point to the potential of leveraging plant autoimmune mutants for plant protection. Although NHP plays a critical role in plant immunity, the disruption of its biosynthesis in the *pmr4/gsl5* mutant background still resulted in stronger basal and pathogen-induced *PR1* gene expression than in WT (Fig. 8). This is likely due to the enhanced and redundant roles of SA, as the increased *PR1* expression was suppressed by the simultaneous disruption of both *SID2* and *FMO1* in the *gsl5-1 fmo1 sid2* triple mutant (Fig. 8). Thus, loss of PMR4/GSL5 callose synthase appears to activate or potentiate numerous defense and defense-related pathways that differ in their impacts on plant growth and fitness. Similarly, Arabidopsis *mlo2* mutants display both early senescence and enhanced powdery mildew resistance (Consonni et al. 2006). Disruption of *PAD4* or SA biosynthetic and signaling genes can alleviate the growth defects without compromising the powdery mildew resistance in the *mlo2* mutants (Consonni et al. 2006). Further molecular dissection of the defense pathways activated in these autoimmune mutants through genetic and molecular approaches could facilitate the strategic deployment of specific defense mechanisms, thereby enabling the development of disease-resistant plants with minimal fitness costs.

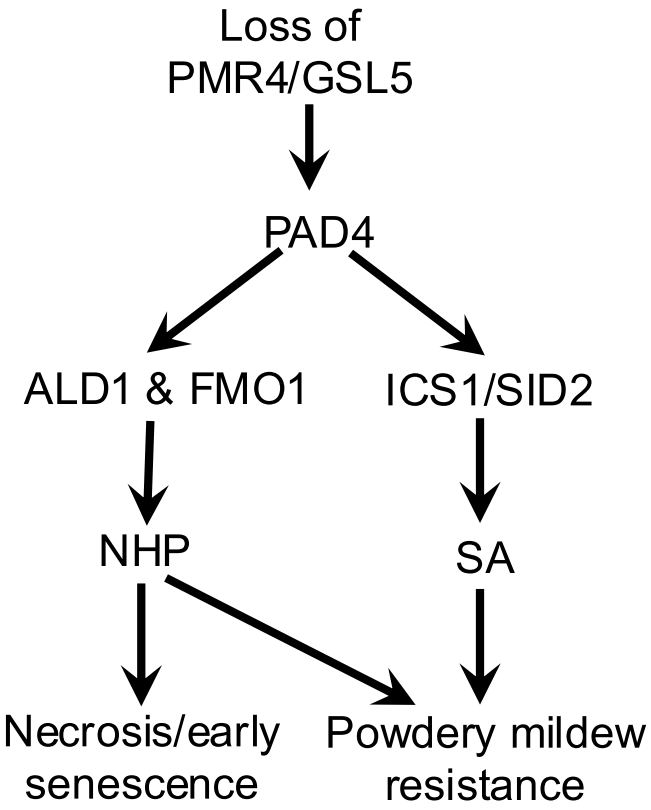

Figure 9. Distinct and overlapping roles of NHP and SA in the autoimmunity of the *pmr4/gsl15* mutants. Loss of PMR4/GSL5 activates PAD4-dependent defense pathways, leading to the induction of NHP and SA biosynthetic genes and their accumulation. Elevated NHP levels play a key role in the necrosis and early senescence of *pmr4/gsl5* mutants, while both SA and NHP have overlapping roles in the powdery mildew resistance of the mutants.

Materials and methods

Plant materials and growth conditions

Arabidopsis (*Arabidopsis thaliana*) WT and mutant plants used in the study are all in the *Col-0* background. Homozygous T-DNA insertion mutants *gsl5-1* (GABI_089H05), *pad4-5* (Salk_206548C), *ald1* (SALK_007673), *fmo1* (SALK_026163), *sid2* (Salk_133146), and *npr1* (SALK_204100) were identified by PCR using primers flanking the T-DNA insertions listed in Supplementary Table S1. The *pmr4-1* mutant and *nahG*-expressing *pmr4-1* line have been previously described (Nishimura et al. 2003). Arabidopsis were grown in growth chambers or rooms at 24 °C, 60 μmol $m^{-2}s^{-1}$ light on a photoperiod of 12-h light and 12-h dark.

Chemical mutagenesis, suppressor screens and mapping by BSA-NGS

EMS mutagenesis of Arabidopsis *gsl5-1* seeds was performed as previously described (Weigel and Glazebrook 2006). In brief, ~50,000 *gsl5-1* mutant seeds were treated with 0.2% EMS for 15 h. EMS-mutagenized seeds were grown in soil and M2 seeds were harvested in pools. Approximately 20,000 M2 seeds were screened and strong extragenic, recessive *spm* mutants without growth or early senescence phenotypes were isolated for further analysis from EMS-mutagenized *gsl5-1* plants at the M2 generation. BSA-NGS was used to identify the *spm* genes (Hua et al. 2017). A *gsl5-1 spm* suppressor mutant was first crossed with the *gsl5-1* mutant to generate the F1 progeny and, subsequently, the F2 segregation population. From the F2 mapping population, individual plants with strong *gsl5-1* lesion/early senescence phenotype or with no lesion/normal senescence phenotype were identified at the 9 to 10th wk postgermination. Leaf samples were collected from 50 to 60 plants of each phenotype and pooled. Genomic DNA was extracted from the pooled samples and used for preparation of libraries and genome sequencing. The sequencing data was subjected to quality control and alignment to the Arabidopsis TAIR10 genome for identification of SNPs and Indels, and for calculation of variant allele frequencies, which were used to identify the chromosome regions for the causative *spm* genes. The genes containing protein-changing SNPs or Indels within the mapping intervals were identified and further confirmed as *SPM* genes through genetic analysis using T-DNA insertion mutants.

Quantification of pipecolic acid

Leaf tissues (~100 mg) were ground in liquid nitrogen in a centrifuge tube. To each sample, 500 μl 90% acetonitrile and 10 μL internal standard DL-pipecolic acid-d9 (10 ng/μL) (LGC Standards, Teddington, UK) were added. The samples were vortexed vigorously for 1 min and centrifuged at 15,000 rpm for 10 min. The clear supernatant was transferred to the wells of a microplate for quantification of pipecolic acid by high-performance liquid chromatography-tandem MS (HPLC-MS/MS) as previously described (Semeraro et al. 2015). Briefly, an Agilent 1,290 Infinity II LC system coupled with an Agilent 6,470 series QQQ MS/MS was used to analyze pipecolic acid (Agilent Technologies, Santa Clara, CA, USA). An Imtakt Intrada Amino Acid column (2.0 mm × 150 mm, 3.0 μm; Imtakt Corporation USA, Portland, OR, USA) was used for LC separation. The buffers were (A) acetonitrile + 0.3% formic acid and (B) acetonitrile/100 mM ammonium formation (20/80 v/v). The linear LC gradient was as follows: time 0 min, 20% B; time 2.5 min, 20% B; time 5 min, 35% B; time 10 min, 100% B; time 11 min, 100% B; time 11.5 min, 20% B; and time 15 min, 20% B. The flow rate was 0.3 mL/min. Multiple reaction monitoring was used for MS analysis. Data were acquired in positive electrospray ionization (ESI) mode using the following ion transitions for pipecolic acid and d_9-pipecolic acid: 130.3→84.1 (20 V), 56.1 (40 V) and 139.3→93.1 (20 V), 61.1 (40 V). The dwell time was set to 30 ms, cell accelerator voltage was 4 V, and the fragmentor voltage was 80 V. The jet stream ESI interface had a gas temperature of 325 °C, gas flow rate of 9 L/min, nebulizer pressure of 35 psi, sheath gas temperature of 250 °C, sheath gas flow rate of 7 L/min, capillary voltage of 3500 V in positive mode, and nozzle voltage of 1000 V. The ΔEMV voltage was 400 V. Agilent Masshunter Quantitative analysis software was used for data analysis (version 10.1).

SA analysis

Free SA and SA + SAG levels in the leaf samples were determined with a biosensor strain *Acinetobacter* species, *ADPWH_lux*, and calculated based on the SA standard curve constructed using the *sid2* mutant leaf extract as described previously (Defraia et al. 2008).

Assays of powdery mildew resistance

Five-week-old short-day (8 h light, 16 h darkness) grown Arabidopsis WT and mutant plants were inoculated with Arabidopsis-adapted powdery mildew isolate *G. cichoracearum* UCSC1 for assays of powdery mildew resistance. Plant inoculation, scoring of disease symptoms, and quantification of sporulation were performed as previously described (Zhang et al. 2018; Wu et al. 2021).

RT-qPCR

Total RNA isolation, DNase treatment, cDNA synthesis and RT-qPCR using *PR1*-specific primers (5′-ctggggtagcggtgacttgt-3′ and 5′-aactccattgcacgtgttcg-3′) were performed with *ACTIN2* (5′-accagctcttccatcgagaa-3′ and 5′-gggcatctgaatctctcagc-3′) as an internal control as described previously (Fu et al. 2023).

Statistical analyses

Statistical analyses were conducted with R software (version 4.4.1). Duncan's multiple range tests were performed with the package agricolae (https://cran.r-project.org/web/packages/agricolae/).

Accession numbers

Sequence data of the Arabidopsis genes described in this article can be found at The Arabidopsis Information Resource (https://www.arabidopsis.org) under the gene identifiers as follows: PMR4/GSL5(AT4G03550), PAD4(At3G53430), ALD1(AT2G13810), FMO1(AT1G19250), ICS1/SID2(AT1G74710), NPR1(At1g64280), PR1(AT2G14610), ACTIN2 (AT3G18780).

Acknowledgments

We thank the Arabidopsis Resource Center at the Ohio State University for providing the mutants used in the study. We thank other members of the Chen lab for help in genotyping of T-DNA mutants, analysis of pipecolic acid and isolation of RNA, and Caroline Hooks and Frank Coker for help in maintaining growth facilities in the Xiao lab.

Author contributions

Z.C. conceived the original research plans. Z.C. and S.X. supervised the experiments; B.F., Z.L. and Z.C. performed most of the experiments; A.S.J. performed some of the experiments; B.F., Z.L., S.X., and Z.C. analyzed the data; Z.C. wrote the article with contributions from other authors.

Supplementary data

The following materials are available in the online version of this article.

Supplementary Figure S1. Response of WT, *pmr4/gsl5*, *pad4*, *ald1*, *fmo1*, and *sid2* mutants to powdery mildew isolate *G. cichoracearum* UCSC1.

Supplementary Table S1. Primers for genotyping of Arabidopsis T-DNA insertion mutants.

Funding

This work was supported by US National Science Foundation (grants no. IOS1758767 and MCB2241515 to Z.C., and IOS1901566 and IOS2224203 to S.X.).

Conflict of interest statement. None declared.

Data availability

All data are included in the paper and its supplementary files.

References

Bartsch M, Gobbato E, Bednarek P, Debey S, Schultze JL, Bautor J, Parker JE. Salicylic acid-independent ENHANCED DISEASE SUSCEPTIBILITY1 signaling in Arabidopsis immunity and cell death is regulated by the monooxygenase FMO1 and the Nudix hydrolase NUDT7. *Plant Cell*. 2006:18(4):1038–1051. https://doi.org/10.1105/tpc.105.039982

Bernsdorff F, Doring AC, Gruner K, Schuck S, Brautigam A, Zeier J. Pipecolic acid orchestrates plant systemic acquired resistance and defense priming via salicylic acid-dependent and -independent pathways. *Plant Cell*. 2016:28(1):102–129. https://doi.org/10.1105/tpc.15.00496

Boutrot F, Zipfel C. Function, discovery, and exploitation of plant pattern recognition receptors for broad-Spectrum disease resistance. *Annu Rev Phytopathol*. 2017:55(1):257–286. https://doi.org/10.1146/annurev-phyto-080614-120106

Brambilla A, Lenk M, Ghirardo A, Eccleston L, Knappe C, Weber B, Lange B, Imani J, Schaffner AR, Schnitzler JP, *et al.* Pipecolic acid synthesis is required for systemic acquired resistance and plant-to-plant-induced immunity in barley. *J Exp Bot*. 2023:74(10):3033–3046. https://doi.org/10.1093/jxb/erad095

Chen YC, Holmes EC, Rajniak J, Kim JG, Tang S, Fischer CR, Mudgett MB, Sattely ES. N-hydroxy-pipecolic acid is a mobile metabolite that induces systemic disease resistance in Arabidopsis. *Proc Natl Acad Sci U S A*. 2018:115(21):E4920–E4929. https://doi.org/10.1073/pnas.1805291115

Consonni C, Humphry ME, Hartmann HA, Livaja M, Durner J, Westphal L, Vogel J, Lipka V, Kemmerling B, Schulze-Lefert P, *et al.* Conserved requirement for a plant host cell protein in powdery mildew pathogenesis. *Nat Genet*. 2006:38(6):716–720. https://doi.org/10.1038/ng1806

Cui H, Gobbato E, Kracher B, Qiu J, Bautor J, Parker JE. A core function of EDS1 with PAD4 is to protect the salicylic acid defense sector in Arabidopsis immunity. *New Phytol*. 2017:213(4):1802–1817. https://doi.org/10.1111/nph.14302

Defraia CT, Schmelz EA, Mou Z. A rapid biosensor-based method for quantification of free and glucose-conjugated salicylic acid. *Plant Methods*. 2008:4(1):28. https://doi.org/10.1186/1746-4811-4-28

Dongus JA, Parker JE. EDS1 signalling: at the nexus of intracellular and surface receptor immunity. *Curr Opin Plant Biol*. 2021:62:102039. https://doi.org/10.1016/j.pbi.2021.102039

Ellinger D, Naumann M, Falter C, Zwikowics C, Jamrow T, Manisseri C, Somerville SC, Voigt CA. Elevated early callose deposition results in complete penetration resistance to powdery mildew in Arabidopsis. *Plant Physiol*. 2013:161(3):1433–1444. https://doi.org/10.1104/pp.112.211011

Ellinger D, Voigt CA. Callose biosynthesis in Arabidopsis with a focus on pathogen response: what we have learned within the last decade. *Ann Bot*. 2014:114(6):1349–1358. https://doi.org/10.1093/aob/mcu120

Enns LC, Kanaoka MM, Torii KU, Comai L, Okada K, Cleland RE. Two callose synthases, GSL1 and GSL5, play an essential and redundant role in plant and pollen development and in fertility. *Plant Mol Biol*. 2005:58(3):333–349. https://doi.org/10.1007/s11103-005-4526-7

Feehan JM, Wang J, Sun X, Choi J, Ahn HK, Ngou BPM, Parker JE, Jones JDG. Oligomerization of a plant helper NLR requires cell-surface and intracellular immune receptor activation. *Proc Natl Acad Sci U S A*. 2023:120(11):e2210406120. https://doi.org/10.1073/pnas.2210406120

Freh M, Gao J, Petersen M, Panstruga R. Plant autoimmunity-fresh insights into an old phenomenon. *Plant Physiol*. 2022:188(3):1419–1434. https://doi.org/10.1093/plphys/kiab590

Fu Y, Fan B, Li X, Bao H, Zhu C, Chen Z. Autophagy and multivesicular body pathways cooperate to protect sulfur assimilation and chloroplast functions. *Plant Physiol*. 2023:192(2):886–909. https://doi.org/10.1093/plphys/kiad133

Hartmann M, Zeier J. N-hydroxypipecolic acid and salicylic acid: a metabolic duo for systemic acquired resistance. *Curr Opin Plant Biol*. 2019:50:44–57. https://doi.org/10.1016/j.pbi.2019.02.006

Hartmann M, Zeier T, Bernsdorff F, Reichel-Deland V, Kim D, Hohmann M, Scholten N, Schuck S, Brautigam A, Holzel T, *et al*. Flavin monooxygenase-generated N-hydroxypipecolic acid is a critical element of plant systemic immunity. *Cell*. 2018:173(2): 456–469.e416. https://doi.org/10.1016/j.cell.2018.02.049

He Z, Webster S, He SY. Growth-defense trade-offs in plants. *Curr Biol*. 2022:32(12):R634–R639. https://doi.org/10.1016/j.cub.2022.04.070

Heck S, Grau T, Buchala A, Metraux JP, Nawrath C. Genetic evidence that expression of NahG modifies defence pathways independent of salicylic acid biosynthesis in the Arabidopsis-Pseudomonas syringae pv. tomato interaction. *Plant J*. 2003:36(3):342–352. https://doi.org/10.1046/j.1365-313X.2003.01881.x

Holmes EC, Chen YC, Mudgett MB, Sattely ES. Arabidopsis UGT76B1 glycosylates N-hydroxy-pipecolic acid and inactivates systemic acquired resistance in tomato. *Plant Cell*. 2021:33(3):750–765. https://doi.org/10.1093/plcell/koaa052

Hua J, Wang S, Sun Q. Mapping and cloning of chemical induced mutations by whole-genome sequencing of bulked segregants. *Methods Mol Biol*. 2017:1578:285–289. https://doi.org/10.1007/978-1-4939-6859-6_24

Huang W, Wang Y, Li X, Zhang Y. Biosynthesis and regulation of salicylic acid and N-hydroxypipecolic acid in plant immunity. *Mol Plant*. 2020:13(1):31–41. https://doi.org/10.1016/j.molp.2019.12.008

Huibers RP, Loonen AE, Gao D, Van den Ackerveken G, Visser RG, Bai Y. Powdery mildew resistance in tomato by impairment of SlPMR4 and SlDMR1. *PLoS One*. 2013:8(6):e67467. https://doi.org/10.1371/journal.pone.0067467

Jacobs AK, Lipka V, Burton RA, Panstruga R, Strizhov N, Schulze-Lefert P, Fincher GB. An Arabidopsis callose synthase, GSL5, is required for wound and papillary callose formation. *Plant Cell*. 2003:15(11): 2503–2513. https://doi.org/10.1105/tpc.016097

Jirage D, Tootle TL, Reuber TL, Frost LN, Feys BJ, Parker JE, Ausubel FM, Glazebrook J. Arabidopsis thaliana PAD4 encodes a lipase-like gene that is important for salicylic acid signaling. *Proc Natl Acad Sci U S A*. 1999:96(23):13583–13588. https://doi.org/10.1073/pnas.96.23.13583

Joglekar S, Suliman M, Bartsch M, Halder V, Maintz J, Bautor J, Zeier J, Parker JE, Kombrink E. Chemical activation of EDS1/PAD4 signaling leading to pathogen resistance in Arabidopsis. *Plant Cell Physiol*. 2018:59(8):1592–1607. https://doi.org/10.1093/pcp/pcy106

Jones JD, Dangl JL. The plant immune system. *Nature*. 2006:444(7117): 323–329. https://doi.org/10.1038/nature05286

Jones JDG, Staskawicz BJ, Dangl JL. The plant immune system: from discovery to deployment. *Cell*. 2024:187(9):2095–2116. https://doi.org/10.1016/j.cell.2024.03.045

Karasov TL, Chae E, Herman JJ, Bergelson J. Mechanisms to mitigate the trade-off between growth and defense. *Plant Cell*. 2017:29(4): 666–680. https://doi.org/10.1105/tpc.16.00931

Kim MG, da Cunha L, McFall AJ, Belkhadir Y, DebRoy S, Dangl JL, Mackey D. Two Pseudomonas syringae type III effectors inhibit RIN4-regulated basal defense in Arabidopsis. *Cell*. 2005:121(5): 749–759. https://doi.org/10.1016/j.cell.2005.03.025

Li P, Lu YJ, Chen H, Day B. The lifecycle of the plant immune system. *CRC Crit Rev Plant Sci*. 2020:39(1):72–100. https://doi.org/10.1080/07352689.2020.1757829

Li R, Maioli A, Yan Z, Bai Y, Valentino D, Milani AM, Pompili V, Comino C, Lanteri S, Moglia A, *et al*. CRISPR/Cas9-based knockout of the PMR4 gene reduces susceptibility to late blight in two tomato cultivars. *Int J Mol Sci*. 2022:23(23):14542. https://doi.org/10.3390/ijms232314542

Lim GH. Regulation of salicylic acid and N-hydroxy-pipecolic acid in systemic acquired resistance. *Plant Pathol J*. 2023:39(1):21–27. https://doi.org/10.5423/PPJ.RW.10.2022.0145

Löwe M, Jürgens K, Zeier T, Hartmann M, Gruner K, Müller S, Yildiz I, Perrar M, Zeier J. N-hydroxypipecolic acid primes plants for enhanced microbial pattern-induced responses. *Front Plant Sci*. 2023:14:1217771. https://doi.org/10.3389/fpls.2023.1217771

Manacorda CA, Mansilla C, Debat HJ, Zavallo D, Sanchez F, Ponz F, Asurmendi S. Salicylic acid determines differential senescence produced by two Turnip mosaic virus strains involving reactive oxygen species and early transcriptomic changes. *Mol Plant Microbe Interact*. 2013:26(12):1486–1498. https://doi.org/10.1094/MPMI-07-13-0190-R

Morris K, MacKerness SA, Page T, John CF, Murphy AM, Carr JP, Buchanan-Wollaston V. Salicylic acid has a role in regulating gene expression during leaf senescence. *Plant J*. 2000:23(5): 677–685. https://doi.org/10.1046/j.1365-313x.2000.00836.x

Nair A, Goyal I, Voss E, Mrozek P, Prajapati S, Thurow C, Tietze L, Tittmann K, Gatz C. N-hydroxypipecolic acid-induced transcription requires the salicylic acid signaling pathway at basal SA levels. *Plant Physiol*. 2021:187(4):2803–2819. https://doi.org/10.1093/plphys/kiab433

Navarova H, Bernsdorff F, Doring AC, Zeier J. Pipecolic acid, an endogenous mediator of defense amplification and priming, is a critical regulator of inducible plant immunity. *Plant Cell*. 2012:24(12):5123–5141. https://doi.org/10.1105/tpc.112.103564

Nawrath C, Metraux JP. Salicylic acid induction-deficient mutants of Arabidopsis express PR-2 and PR-5 and accumulate high levels of camalexin after pathogen inoculation. *Plant Cell*. 1999:11(8): 1393–1404. https://doi.org/10.1105/tpc.11.8.1393

Nishimura MT, Stein M, Hou BH, Vogel JP, Edwards H, Somerville SC. Loss of a callose synthase results in salicylic acid-dependent disease resistance. *Science*. 2003:301(5635):969–972. https://doi.org/10.1126/science.1086716

Santillan Martinez MI, Bracuto V, Koseoglou E, Appiano M, Jacobsen E, Visser RGF, Wolters AA, Bai Y. CRISPR/Cas9-targeted mutagenesis of the tomato susceptibility gene PMR4 for resistance against powdery mildew. *BMC Plant Biol*. 2020:20(1):284. https://doi.org/10.1186/s12870-020-02497-y

Semeraro M, Muraca M, Catesini G, Inglese R, Iacovone F, Barraco GM, Manco M, Boenzi S, Dionisi-Vici C, Rizzo C. Determination of plasma pipecolic acid by an easy and rapid liquid chromatography-tandem mass spectrometry method. *Clin Chim Acta*. 2015:440:108–112. https://doi.org/10.1016/j.cca.2014.11.014

Shields A, Shivnauth V, Castroverde CDM. Salicylic acid and N-hydroxypipecolic acid at the fulcrum of the plant immunity-growth equilibrium. *Front Plant Sci*. 2022:13:841688. https://doi.org/10.3389/fpls.2022.841688

Smith LM. Salicylic acid, senescence, and heterosis. *Plant Physiol*. 2019:180(1):3–4. https://doi.org/10.1104/pp.19.00260

Stone BA, Clarke AC. *Chemistry and biology of (1->3)-b-glucans*. Bundoora, Victoria: La Trobe University Press; 1992.

Tan Q, Zhao M, Gao J, Li K, Zhang M, Li Y, Liu Z, Song Y, Lu X, Zhu Z, *et al*. AtVQ25 promotes salicylic acid-related leaf senescence by fine-tuning the self-repression of AtWRKY53. *J Integr Plant Biol*. 2024:66(6):1126–1147. https://doi.org/10.1111/jipb.13659

van Wees SC, Glazebrook J. Loss of non-host resistance of Arabidopsis NahG to Pseudomonas syringae pv. phaseolicola is due to degradation products of salicylic acid. *Plant J*. 2003:33(4): 733–742. https://doi.org/10.1046/j.1365-313X.2003.01665.x

van Wersch R, Li X, Zhang Y. Mighty dwarfs: arabidopsis autoimmune mutants and their usages in genetic dissection of plant

immunity. *Front Plant Sci*. 2016:7:1717. https://doi.org/10.3389/fpls.2016.01717

Vogel J, Somerville S. Isolation and characterization of powdery mildew-resistant Arabidopsis mutants. *Proc Natl Acad Sci U S A*. 2000:97(4):1897–1902. https://doi.org/10.1073/pnas.030531997

Wang Y, Li X, Fan B, Zhu C, Chen Z. Regulation and function of defense-related callose deposition in plants. *Int J Mol Sci*. 2021:22(5):2393. https://doi.org/10.3390/ijms22052393

Wang Y, Schuck S, Wu J, Yang P, Doring AC, Zeier J, Tsuda K. A MPK3/6-WRKY33-ALD1-pipecolic acid regulatory loop contributes to systemic acquired resistance. *Plant Cell*. 2018:30(10):2480–2494. https://doi.org/10.1105/tpc.18.00547

Wang Z, Li X, Wang X, Liu N, Xu B, Peng Q, Guo Z, Fan B, Zhu C, ChenZ. Arabidopsis endoplasmic Reticulum-localized UBAC2 proteins interact with PAMP-INDUCED COILED-COIL to regulate pathogen-induced callose deposition and plant immunity. *Plant Cell*. 2019:31(1):153–171. https://doi.org/10.1105/tpc.18.00334

Weigel D, Glazebrook J. *EMS mutagenesis of Arabidopsis seed*. CSH Protoc; 2006.

Wu Y, Diaz D, Yin J, Bloodgood D, Sexton W, Wei CI, Xiao S. An easy and flexible inoculation method for accurately assessing powdery mildew-infection phenotypes of Arabidopsis and other plants. *J Vis Exp*. 2021:169. https://doi.org/10.3791/62287

Yildiz I, Mantz M, Hartmann M, Zeier T, Kessel J, Thurow C, Gatz C, Petzsch P, Kohrer K, Zeier J. The mobile SAR signal N-hydroxypipecolic acid induces NPR1-dependent transcriptional reprogramming and immune priming. *Plant Physiol*. 2021:186(3):1679–1705. https://doi.org/10.1093/plphys/kiab166

Yoshimoto K, Jikumaru Y, Kamiya Y, Kusano M, Consonni C, Panstruga R, Ohsumi Y, Shirasu K. Autophagy negatively regulates cell death by controlling NPR1-dependent salicylic acid signaling during senescence and the innate immune response in Arabidopsis. *Plant Cell*. 2009:21(9):2914–2927. https://doi.org/10.1105/tpc.109.068635

Zavaliev R, Dong XN. NPR1, a key immune regulator for plant survival under biotic and abiotic stresses. *Mol Cell*. 2024:84(1):131–141. https://doi.org/10.1016/j.molcel.2023.11.018

Zhang B, Huang S, Guo Z, Meng Y, Li X, Tian Y, Chen W. Salicylic acid accelerates carbon starvation-induced leaf senescence in Arabidopsis thaliana by inhibiting autophagy through nonexpressor of pathogenesis-related genes 1. *Plant Sci*. 2023:336:111859. https://doi.org/10.1016/j.plantsci.2023.111859

Zhang C, Xie Y, He P, Shan L. Unlocking Nature's defense: plant pattern recognition receptors as guardians against pathogenic threats. *Mol Plant Microbe Interact*. 2024:37(2):73–83. https://doi.org/10.1094/MPMI-10-23-0177-HH

Zhang D, Zhu Z, Gao J, Zhou X, Zhu S, Wang X, Wang X, Ren G, Kuai B. The NPR1-WRKY46-WRKY6 signaling cascade mediates probenazole/salicylic acid-elicited leaf senescence in Arabidopsis thaliana. *J Integr Plant Biol*. 2021:63(5):924–936. https://doi.org/10.1111/jipb.13044

Zhang Q, Berkey R, Blakeslee JJ, Lin J, Ma X, King H, Liddle A, Guo L, Munnik T, Wang X, *et al.* Arabidopsis phospholipase Dalpha1 and Ddelta oppositely modulate EDS1- and SA-independent basal resistance against adapted powdery mildew. *J Exp Bot*. 2018:69(15):3675–3688. https://doi.org/10.1093/jxb/ery146

Zhang Y, Wang HL, Li Z, Guo H. Genetic network between leaf senescence and plant immunity: crucial regulatory nodes and new insights. *Plants (Basel)*. 2020:9(4):495. https://doi.org/10.3390/plants9040495

Zheng ZY, Qualley A, Fan BF, Dudareva N, Chen ZX. An important role of a BAHD acyl transferase-like protein in plant innate immunity. *Plant J*. 2009:57(6):1040–1053. https://doi.org/10.1111/j.1365-313X.2008.03747.x

Zhou N, Tootle TL, Tsui F, Klessig DF, Glazebrook J. PAD4 functions upstream from salicylic acid to control defense responses in Arabidopsis. *Plant Cell*. 1998:10(6):1021–1030. https://doi.org/10.1105/tpc.10.6.1021